Bioelectrochemistry 149 (2023) 108323

Contents lists available at ScienceDirect

Bioelectrochemistry

journal homepage: www.journals.elsevier.com/bioelectrochemistry

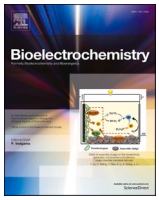

Square wave voltammetric study of interaction between 9-acridinyl amino acid derivatives and DNA

Jelena Rupar [a], Vladimir Dobričić [b], Jasmina Brborić [b], Olivera Čudina [b], Mara M. Aleksić [a,*]

[a] University of Belgrade – Faculty of Pharmacy, Department of Physical Chemistry and Instrumental Methods, Vojvode Stepe 450, P.O. Box 146, 11221 Belgrade, Serbia
[b] University of Belgrade – Faculty of Pharmacy, Department of Pharmaceutical Chemistry, Vojvode Stepe 450, P.O. Box 146, 11221 Belgrade, Serbia

ARTICLE INFO

Keywords:
9-acridinyl amino acid derivatives
DNA-electrochemical biosensor
Interaction
Square wave voltammetry
Molecular docking

ABSTRACT

Electrochemical oxidation of newly synthesized acridine derivatives (ADs): PG, PA, EG and EA was studied using square wave voltammetry at a glassy carbon electrode. Oxidation occurs as an irreversible process for all ADs. The ADs interaction with DNA was investigated using multi-layer DNA electrochemical biosensor. The shift of dA peak in positive direction indicated that the type of interaction is most likely an intercalation. PG showed the widest range of concentration capable to interact with DNA (1×10^{-7} M – 2.5×10^{-4} M). Analysing $\log\left[\frac{I_{complex}}{I_{DNA}-I_{complex}}\right]$ *vs* $\log c_{AD}$ plots, the binding constants were determined. For the lowest PG concentrations, obtained *K* value close to 10^6 M^{-1} refers to strong binding. The values of *K* for PA may be classified as medium strength, while EG and EA showed low *K* values. Our results unequivocally showed that the characteristics of association complexes may vary depending on the concentration of the interacting substance. The negative ΔG value for all ADs, (– 21 to – 34 kJ mol^{-1}), confirms the process spontaneity. The best result, indicating the most stable formed complex with DNA adsorbed at the electrode surface, showed PG when present in low concentration, order of 10^{-7} M. The intercalation of ADs into DNA was supported by molecular docking analysis.

1. Introduction

Acridines are molecules which found usage in industry as well in medicine, as antibacterial, antiviral, anti-inflammatory and antitumor agents [1]. Their property to intercalate between base pairs in the deoxyribonucleic acid (DNA) structure makes them good candidates for cancer treatment [2]. Beside intercalation - the most common non-covalent binding mode of small molecules with DNA, groove binding and outer electrostatic binding, are also reported as interaction modes of some acridines with DNA [3].

Amino acid acridine derivatives are of special interest due to their different mechanisms of action which results in significant antitumor activity. Acridone substituted with amino acids were investigated with the aim to determine the anticancer activity of the new compounds, and synthesized derivatives had significant antiproliferative activity towards C6 Glioma cells as a result of arrest cells in G_0/G_1 phase of the cell cycle [4]. 9(10*H*)-acridinone derivatives with amino substituents at *C*2 position on the acridinone ring were cytotoxic to leucemia cells according to their significant binding to DNA and cell growth inhibition [5]. Authors Wang et all. [6] explored different mechanisms of action of acridone derivatives with amino acids substituents at *C*2 and confirmed multiple mechanisms of action such as: aerobic glycolysis suppression, mitochondrial oxidative phosphorylation, DNA damage and oxidative stress.

Lyakhov et al. synthesized and investigated 9-acridine amino acid derivatives. They established that the selected amino acid and the number of methyl groups in its side chain influenced its cytotoxic activity [7]. *In vitro* anticancer activity including: cytotoxicity, cell cycle influence, cell death and topoisomerase II α inhibitory effect, of acridine derivatives (ADs) substituted in position C9 with different methyl and ethyl esters of amino acids, was evaluated by our research team. Most active compounds with aliphatic amino acid esters showed good cytotoxic activity against A549 and lack of toxicity towards normal human leucocytes [8].

As the effect on DNA is one of the most important actions of a potential antitumor agent, in this paper we have examined the interaction of selected synthetized compounds with DNA.

Voltammetry was used with aim to determine the type of non-covalent interaction and for calculating the binding constants due to

* Corresponding author at: University of Belgrade – Faculty of Pharmacy, Department of Physical Chemistry and Instrumental Methods, Vojvode Stepe 450, P.O. Box 146, 11221 Belgrade, Serbia.
E-mail address: mara.aleksic@pharmacy.bg.ac.rs (M.M. Aleksić).

https://doi.org/10.1016/j.bioelechem.2022.108323
Received 7 September 2022; Received in revised form 27 October 2022; Accepted 7 November 2022
Available online 11 November 2022

its advantage over UV–vis spectrometry, fluorescence and electrophoresis. The main advantage of electrochemical over other techniques is its ability to measure and determine the binding constants over a wider range of concentration [9], also the low cost, higher speed of analysis, and high reliability make it the method of choice. As it requires small number of samples, and low amount of investigated compounds for interaction with DNA, it is increasingly used for newly synthesized compounds analysis.

Electrochemical DNA biosensors are most frequently used for *in situ* investigation of the interaction. Regarding to different immobilization procedure and consequently different morphology of the adsorbed layer, there are three different biosensors when the DNA molecule is a recognition molecule: thin-layer, thick-layer and multi-layer biosensor. Thin-layer DNA-biosensor is formed after immersing the electrode in DNA solution and applying positive potential during predetermined time for optimal output. Thick-layer DNA-biosensor is formed by covering the electrode surface with DNA solution of rather high concentration (above 30 mg mL^{-1}) and drying under normal atmosphere [3,10]. Multi-layer biosensor is formed by consecutively covering the electrode surface with several drops (usually-three) of lower concentration DNA solution (below 100 μg mL^{-1}), where after each drop, the electrode surface dries under the nitrogen atmosphere [11–13]. Multi-layer biosensor and thick-layer biosensor enable the complete coverage of the electrode surface by DNA but the time required for multi-layer biosensor construction is shorter, and lower DNA concentration is needed, thus this biosensor was used in this study [3].

Most often used voltammetric technique for biosensor investigation is differential pulse voltammetry (DPV) but square wave voltammetry (SWV) has its benefits. SWV analysis is performed with higher speed (lasting 1–30 s) comparing to DPV (2–4 min) as a consequence of high effective scan rate, as well as with greater response and lower consumption of electroactive species [14]. Increased repetitiveness and the signal-to-noise ratio are also the reasons for using the SWV instead DPV [14]. Based on the change in oxidation signal of DNA nucleosides (deoxyadenosine (dA) and deoxyguanosine (dG)) in the presence of reacting substance, the appearance and the mode of the interaction can be confirmed. Also, 8-oxoguanine (8-oxoG) and 2,8-dihydroxyadenine (2,8-DHA), substances known as strong mutagen agents formed as a result of oxidative stress, can be detected in the voltammogram [15]. The absence of these peaks indicates that the compound of interest causes no oxidative damage to DNA.

In this study, the interaction of ADs synthesized in our laboratory in accordance with the procedure previously published by Lyakhov et al. [7] (Propyl 4-(acridin-9-ylamino)butanoate (PG), Propyl 3-(acridin-9-ylamino)propanoate (PA), Ethyl 4-(acridin-9-ylamino)butanoate (EG) and Ethyl 3-(acridin-9-ylamino)propanoate (EA) (Scheme 1)) with DNA was investigated. Among a larger number of synthesized acridine derivatives, these four compounds seems to be the most promising anticancer candidates, since they were proved to be the most potent viability inhibitors in cancer cells, where toxicity towards unstimulated normal human leucocytes was not noticed [8].

To estimate the strength of the interaction, i.e. for calculating the binding constants (K) of complex formed between small molecules and DNA using voltammetry, usually small molecules are titrated by DNA and their redox current decrease, in the presence of increasing DNA amount, is considered [9,16,17]. In the case of present study, the necessary modifications were applied due to the biosensor multi-layer structure, and constant DNA amount attached to the electrode surface. Therefore, the investigations were done using the increased concentration of acridine derivatives [18] and measuring the square wave voltammetric peak current intensity of deoxyadenosine oxidation. SWV was the method of choice to examine and compare the interaction of synthetized ADs with DNA since K values vary depending on the difference in the structure of selected amino acid ester, as well as its chain length.

Interaction of newly synthesized compounds with DNA would supplement information on their mechanism of action, with respect of previously obtained electrophoretic mobility shift assay results [8], which implied that PG intercalated into DNA.

The aim of this work was to clarify the oxidation of newly synthesized compounds with potential anticancer activity at a glassy carbon electrode (GCE) using SWV, to evaluate the binding constants of the formed adsorbed association complex and to determine the mode of interaction of compounds with DNA. Based on obtained results, the scope will be to determine the particular AD which interacts with DNA at lowest concentrations, has the highest affinity, and form the most stable complex with DNA. Molecular docking analysis will be used in order to support the experimental information.

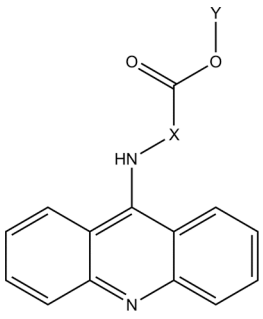

	X	Y
PG	$-CH_2CH_2CH_2-$	$-CH_2CH_2CH_3$
PA	$-CH_2-CH_2-$	$-CH_2CH_2CH_3$
EG	$-CH_2CH_2CH_2-$	$-CH_2CH_3$
EA	$-CH_2-CH_2-$	$-CH_2CH_3$

Scheme 1. Structure of acridine derivatives.

2. Experimental

2.1. Apparatus

For voltammetric measurements a μAutolab analyser operating with GPES 4.9 software (Eco Chemie, Utrecht, The Netherlands) was used. In three electrode cell, GCE (d = 3 mm, CH Instruments, Inc., Austin, TX, USA) was used as a working electrode, Ag/AgCl as a reference (3.00 M KCl) and Pt as an auxiliary electrode. Before each measurement, GCE was polished on a smooth polishing pad with aqueous slurry of Al_2O_3 powder (particle size 0.05 μm). After polishing, the GCE was sonicated for two minutes in double distilled water and absolute ethanol, respectively. Sonication was performed in an ultrasonic bath 'Iskra' UZ 4R (Sentjernej, Slovenia), and pH measurements were carried out with a PHM 220 pH meter with a combined electrode Radiometer GK2401B. For weight measurements a SCALTEC SBC 31 balance was used.

UV–vis spectrophotometric measurement was conducted using Thermo Scientific™ GENESYS™ UV–vis Spectrophotometer with VISIONlite™ software, and Fluorimetric measurements were conducted using Thermo Scientific™ Invitrogen™ Qubit™ 4 Fluorometer with Qubit™ dsDNA HS Assay Kit.

2.2. Reagents

9-acridinyl amino acid derivatives (AD): propyl 4-(acridin-9-ylamino)butanoate (PG), propyl 3-(acridin-9-ylamino)propanoate (PA), ethyl 4-(acridin-9-ylamino)butanoate (EG) and ethyl 3-(acridin-9-ylamino)propanoate (EA) were synthesized in our laboratory, using a two-step procedure [7,8]. In the first step, an alcohol solution of 9-chloroacridine was mixed with a solution of alkoxide and refluxed for 2.5 h, and in the second step the appropriate amino acid was added into the reaction mixture and the reflux was continued. The 1.0×10^{-3} M stock solutions of synthesized ADs (PG, PA, EG and EA) were prepared in absolute ethanol and stored at 4 °C.

Deoxyribonucleic acid sodium salt from calf thymus (Calf thymus DNA (CT-DNA) Product Number D 1501) was obtained from Sigma-Aldrich. The stock solution of DNA, 73.95 μg mL^{-1} was prepared by dissolving in 0.1 M acetate buffer, pH 4.6.

The fraction of dsDNA in prepared control solution was evaluated by two methods, UV–vis spectrophotometry and fluorimetry (Qubit™

dsDNA HS Assay Kit, Invitrogen).

By comparing the results obtained by these two techniques (the first of which determines total concentration of all molecular species that contain nucleic bases [19], and the second only the dsDNA fraction [20] the DNA solution contained about 75 % dsDNA, while other 25 % may contain short or long single stranded DNA, polynucleotide chains and other DNA fragments.

The DNA molecular weight of the sample used in the study was validated by agarose gel electrophoresis. DNA sample was diluted under three different conditions (in acetate buffer pH 4.6, 0.1 M used in this work; phosphate buffer pH 6.9, 0.1 M and phosphate buffer pH 6.9, 0.01 M) and ran in a 1 % agarose gel (Fig. S1, in the Supplementary Material). In agreement with the results obtained by Qubit BR dsDNA assay, the dominant fraction is above 10 kb corresponding to intact dsDNA, with a smear down to 1.5 kb indicating degraded dsDNA and/or ssDNA. Compared to DNA sample dissolved in neutral solution of the same ionic strength, our working solution did not differ significantly; while the sample in the solution of lower ionic strength seems to be more degraded as observed with smear down to 1.0 kb.

All experiments were done in pH 4.6, 0.1 M acetate buffer at room temperature (25 ± 1 °C).

The electrolyte solution of acetate buffer pH 4.6 was prepared according to the literature [21] as sodium acetate in the solution of acetic acid using analytical grade reagents and double distilled water. To eliminate the oxygen from the solution, high purity nitrogen gas was passing through the solution for 10 min before the measurement, and flowing over the solution during the voltammetric measurements.

2.3. Preparation of the biosensor

Before using, the GCE was polished with alumina slurry to obtain a mirror-like surface. After washing and drying, 5 μL drop of DNA stock solution (73.95 μg mL^{-1}) was dropped at the clean surface and allowed to dry for 30 min under an atmosphere of nitrogen. This procedure was repeated three times and eventually the multi-layer DNA biosensor was prepared after covering the GCE surface successively with the third drop of DNA solution. After the last drop was dried, to avoid the nonspecific adsorption, the excess of unbounded DNA molecules was eliminated from the biosensor surface by washing with deionized water [18]. Immediately after the preparation, biosensor was transferred to the AD solution for incubation, after which it was washed off with deionized water and transferred to the electrochemical cell. For each SWV scan, the newly prepared multi-layer DNA biosensor was used.

Five biosensors were prepared to test the response reproducibility using current and potential measurements. The standard deviation showed satisfactory results being 2–3 mV for peak potential and 8nA for peak current. The sensor response reproducibility was expressed by the relative standard deviation (RSD). The obtained values were 0.18 % and 0.23 % for peak dG and dA potential, and 8.5 % and 4.4 % for peak dG and dA current, respectively. Results are presented in Table S1 in Supplementary Material.

2.4. Voltammetric measurements

Voltammetric measurements were performed using cyclic and SWV. Cyclic voltammetry (CV) was conducted at pH 4.6 in the potential range between –1.5 V and + 1.5 V (*vs* Ag/AgCl, 3 M KCl), always starting from 0.0 V, scanning towards positive potential, as well as in negative (reverse) direction with scan rate of 0.05 V s^{-1} and step potential of 0.005 V.

SWV was applied under the selected conditions: the frequency was 25 Hz, step potential 0.001 V, pulse amplitude of 0.005 V, yielding an effective scan rate of 0.025 V s^{-1}. All SW voltammograms were smoothed using the Savitzky-Golay filter (level 4) and afterwards treated by baseline correction using moving average application with a step window of 5 mV. Data processing was done using the GPES version 4.9 software with the purpose of better and clearer identification of the peaks presented.

For investigations of AD interaction with DNA, multi-layer DNA biosensor was immersed in the solution of each AD and allowed to incubate for 30 min period with different concentration (1×10^{-7} M to 2.5×10^{-4} M) at room temperature. After the incubation, biosensor was removed from the AD solution, washed with deionized water and transferred to the electrochemical cell.

2.5. Molecular docking analysis

Molecular docking studies were carried out using AutoDock Vina [22], whereas final preparation of tested molecules and receptor for docking was performed in AutoDock Tools 1.5.6 [23]. 3D coordinates of the X-ray crystal structure of the ternary complex DNA/topoisomerase II/amsacrine were retrieved from the Protein Data Bank (PDB code: 4g0u) [24]. This file was analyzed in Discovery Studio Visualizer 4.5.0 [25], which was used for the initial preparation of receptor for docking. A grid of 20, 20 and 20 points in x-, y-, and z-direction, respectively, with grid spacing of 0.375 Å was built centered on the center of mass of the catalytic site of considered receptor. The exhaustiveness parameter was set to 8. Validation of the docking procedure was performed by re-docking of the co-crystallized ligand into the 3D structure of the receptor. Obtained RMSD value (<2 Å) confirmed validity of applied docking analysis.

3. Results and discussion

3.1. Oxidation of 9-acridinyl amino acid derivatives at bare GCE

Basic voltammetric study of oxidation process of synthesized acridines PG, PA, EG, and EA on GCE was performed by CV. Fig. 1 shows voltammograms recorded at GCE of 2.4×10^{-4} M PG in nitrogen-saturated acetate buffer pH 4.6. Three successive scans were performed with potentials always starting from 0.0 V (*vs* Ag/AgCl, 3 M KCl) and changing it towards positive (Fig. 1A) and negative (Fig. 1B) potential limits.

With potential cycling from 0.0 V towards + 1.5 V and backward to − 1.5 V, during the first scan (Fig. 1A) one anodic peak (I) at $E_{p,I} \approx 1.0$ V and two cathodic peaks at − 0.75 V and − 1.0 V appeared. In the second and third scan oxidation peak I height decreased. While the peak I was fading, new oxidation peak II arose at about + 0.6 V in the second scan. In another experiment, when the scan direction is changed and the potential was scanned from 0.0 V to − 1.5 V and backward to + 1.5 V (Fig. 1B), PG yielded two cathodic and two anodic peaks in the first scan. It should be noted that in the reverse part of the first cycle anodic peak II appeared at potential of 0.6 V, followed by peak I (at 1.0 V). During the second and third scan peak II increased and stabilized, while peak I decreased.

At the same time, cathodic peaks due to the PG reduction showed the same behaviour as before. In successive scans they were slightly shifted to more negative potentials, and their peak heights decreased.

According to the above results, it may be suggested that the PG reduction product/s are capable of being oxidized yielding a peak II at potential of + 0.6 V. This peak may be observed only with previously applied negative potential, otherwise was absent.

Observing the shape of the voltammograms it is evident that both oxidation and reduction processes are irreversible.

The same situation was observed for other three investigated derivatives, and their CV voltammograms are presented in the Fig. S2, Fig. S3 and Fig. S4 (in the Supplementary Material).

SW voltammograms of 2.4×10^{-4} M acridine derivatives solutions were recorded in the potential range from 0.0 V to 1.5 V *vs* Ag/AgCl (3 M KCl) in 0.1 M acetate buffer pH 4.6, and showed one main oxidation peak (I) at potential about 1.0 V, (Fig. 2, curve 1). When the investigated potential range was extended in the negative direction, starting from −

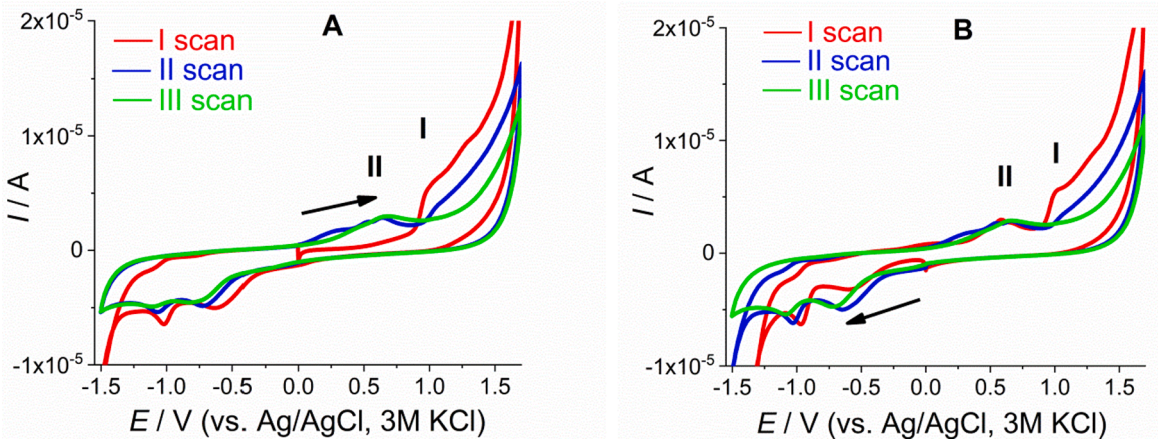

Fig. 1. The CVs of 2.4 × 10^{-4} M PG recorded in acetate buffer pH 4.6, at the potential range between −1.5 V and + 1.5 V, starting from 0.0 V: (A) in the positive direction and (B) in the negative direction; first (——), second (——) and third (——) scan; ν = 50 mV s^{-1}.

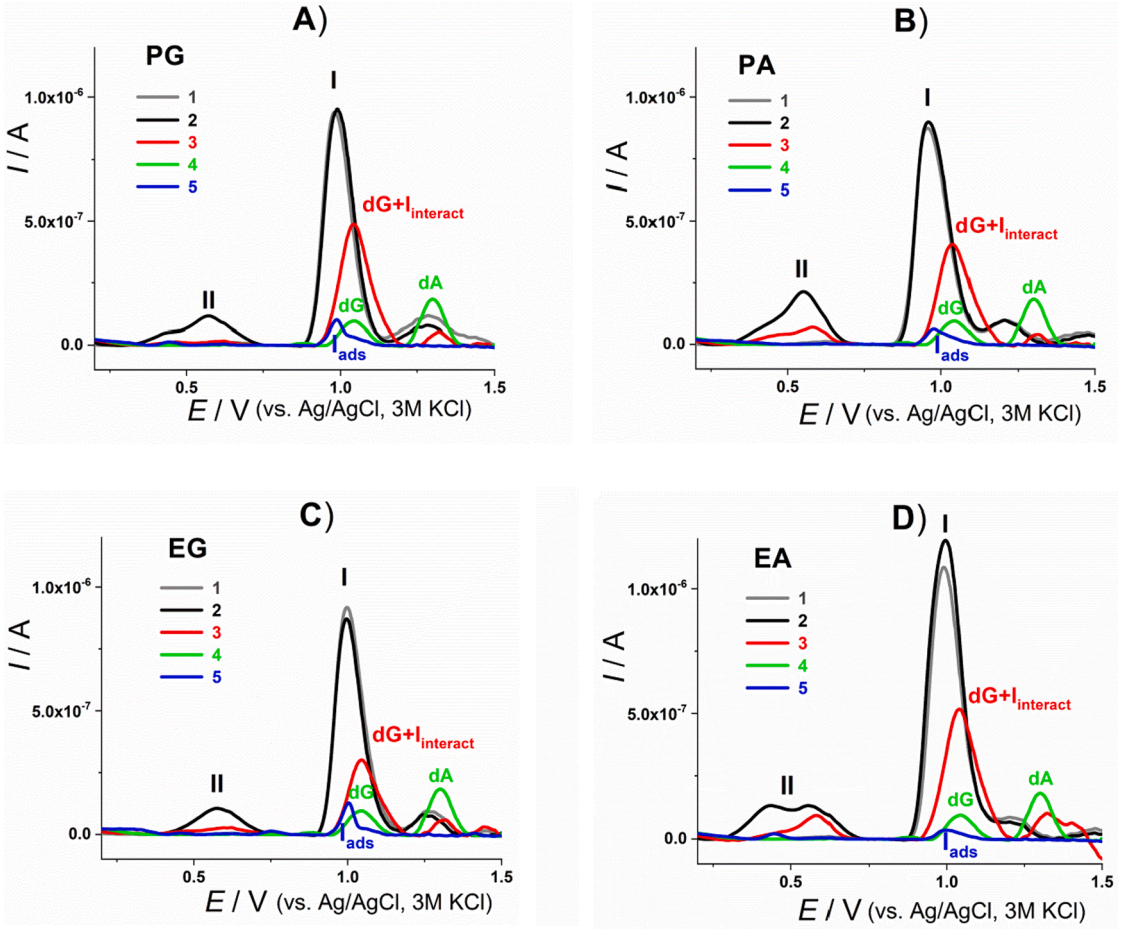

Fig. 2. Corrected SW voltammograms of ADs, DNA and ADs-DNA mixtures: A) PG; B) PA; C) EG and D) EA. All curves were recorded from − 1.4 V to + 1.5 V, except the curve 1 which was recorded from 0.0 V to + 1.5 V, and for visual clearness all curves are graphically presented in the potential range + 0.2 V to + 1.5 V. Curve 1 (——) recorded in the 2.4 × 10^{-4} M AD solution from 0.0 V; curve 2 (——) recorded in the 2.4 × 10^{-4} M AD solution; curve 3 (——) recorded after DNA/GCE incubation in 2.4 × 10^{-4} M AD solution for 30 min; curve 4 (——) recorded after DNA/GCE incubation in acetate buffer pH 4.6 for 30 min; curve 5 (——) recorded after GCE incubation in 2.4 × 10^{-4} M AD solution for 30 min. After the incubation electrode was transferred to acetate buffer pH 4.6, 0.1 M and voltammograms were recorded at f = 25 Hz, Es = 1 mV, pulse amplitude 5 mV; ν_{eff} = 25 mV s^{-1}.

1.4 V towards + 1.5 V, another smaller and very broad oxidation peak (II) was detected at 0.4–0.6 V (Fig. 2, curve 2 - part of the voltammogram recorded from − 1.4 V to 0.2 V is not shown for a clearer graphic display). Since this peak was not present in the first case, it can be suggested that it occurred as an oxidation of the AD`s reduction product formed at the GCE surface during the scan in negative potentials. This finding is in accordance with CV results.

In the SW voltammetric experiment the current was sampled in

positive and negative-going pulses at the same time, so the peaks that correspond to the oxidation and reduction may be obtained at the same time, what is used for reversibility predictions [26,27]. By analysing the forward and backward components of the current, each peak in ADs voltammogram showed irreversible nature since both peak components, as well as the total peak current, were oriented in the same direction [18,28,29]. Fig. 3 shows SW voltammograms of 2.4 × 10^{-4} M PG solution at pH 4.6, *I* 0.1 M where the total current (I_t) together with forward (I_f) and backward (I_b) current components showed peaks oriented in the positive direction. The same situation was recorded for other three ADs (not shown), indicating the irreversible nature of the oxidation process for all synthesized compounds.

In order to obtain the proper response for SWV measurements, the pulse amplitude, step and frequency were optimized to 5 mV, 1 mV and 25 Hz, respectively.

In another experiment the oxidation of PG, PA, EG, and EA was tested after the 30 min period of bare GCE immersed in the acridine derivatives 2.4 × 10^{-4} M solutions, allowing the ADs to adsorb at the electrode surface. After rinsing with water, the electrode was transferred to the electrochemical cell and the recorded SW voltammogram for each compound showed tiny peak (I_{ads}) at potential slightly more positive (3–7 mV) compared to the main peak I in the solution (Fig. 2, curve 5). At the same time peak II was not noticeable. A conspicuous decrease of ADs peak current indicated very weak adsorption at the electrode surface. The decrease of oxidation signal obtained after the adsorption of ADs at the GCE can be presented by normalized peak current (equation (1)), representing a percentage of signal change [18,30,31],

$$d(I)\% = \frac{I_{p,ads}}{I_{p,\,sol}} \times 100 \quad (1)$$

where $I_{p,\,ads}$ represent signal of the peak current obtained after the GCE immersion in the AD solution and transfer to the blank electrolyte for measurement, and $I_{p,sol}$ is the peak current measured for the oxidation of AD in the solution. Peak potentials and values of normalized peak currents for all ADs obtained by using the equation (1) are shown in the Table 1.

Normalized peak current values were between 3 % what was calculated for EA, and 15 % in the case of EG. It indicated that EA showed very little or none affinity to adsorb at the surface of the GCE, while PG, and EG showed moderate adsorption ability.

To be able to predict the number of electrons exchanged at pH 4.6 during the oxidation of ADs, the shape of the oxidation peak was considered. According to the difference between the CV peak potential

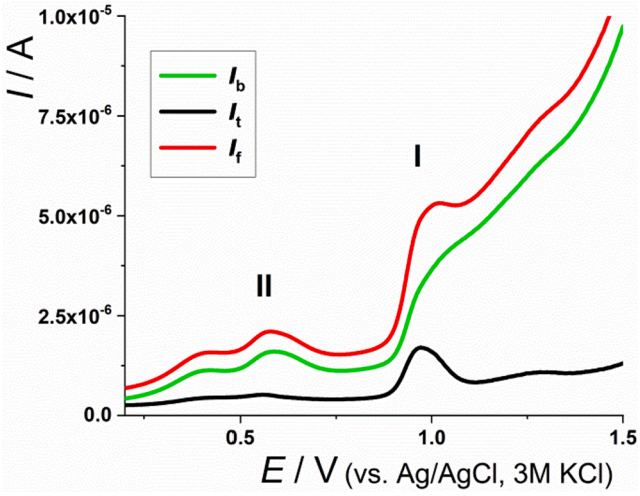

Fig. 3. SW voltammograms obtained with the GCE in 2.4 × 10^{-4} M PG in acetate buffer pH 4.6, 0.1 M; f = 25 Hz, Es = 1 mV, pulse amplitude 5 mV; v_{eff} = 25 mV s^{-1}; I_t - total current, I_f - forward current, I_b - backward current.

Table 1
Peak potentials and normalized peak currents of ADs and AD-DNA SWV signals.

Acridine derivative	$E_{p,sol}$ (V)	$E_{p,ads}$ (V)	ΔE_p (V)	d(*I*) (%)	Interaction with DNA	
					ΔE_p (V) ($E_{p0,dA}$ = 1.301 V)	d(dA) (%)
PG	0.984	0.988	0.004	10.3	0.014	21.75
PA	0.966	0.973	0.007	6.86	0.015	31.61
EG	0.999	1.003	0.004	15.6	0.015	35.22
EA	0.993	0.996	0.003	3.25	0.011	66.77

and half-height peak potential $\left|E_p - E_{p1/2}\right| = 47.7/(\alpha n_\alpha)$, which was between 80 and 100 mV, and the DPV half peak width $W_{1/2} = \frac{3.52RT}{\alpha nF}$, being 120–140 mV (voltammograms not shown) of all investigated compounds, it is calculated that one electron is involved in the oxidation process [32].

The molecular structure of all synthesized derivatives reveals the common acridine polyaromatic planar nitrogen heterocycle, which owing to its available non-bonding electrons on nitrogen can act as an electron donor. According to results presented here, our previous research [18] and other literature data [33,34] it can be assumed that oxidation at about 1.0 V occurs at nitrogen in the position 10, which loses one electron to form a monomer radical cation which can further dimerize. Additional small peak at 0.6 V most probably was a consequence of the oxidation of reduction product formed at the GCE surface during the scan in negative potentials.

3.2. Acridine derivatives interaction with DNA

The interaction between DNA and ADs (PG, PA, EG and EA) was investigated using DNA electrochemical biosensor which consisted of GCE with immobilized DNA network (as described in the sections 2.2 and 2.3.) at its surface. Upon the interaction of investigated compounds in the solution with surface-immobilized DNA, the change in the oxidation signal of DNA occurred as a consequence of changes in the DNA morphology [35].

In SW voltammogram obtained with DNA electrochemical biosensor immersed in acetate buffer pH 4.6, *I* 0.1 M, two peaks representing the oxidation of deoxyguanosine (dG) and deoxyadenosine (dA) [18] appeared at potentials 1.04 V and 1.30 V, respectively (Fig. 2, curve 4). Although pH 7.0 is close to physiological, measurements at pH 4.6 were more convenient because currents were higher and peaks were better shaped [18,36] and therefore the experiments were conducted at pH 4.6. Usually, DPV is used for DNA oxidation studies [37–41], but based on our experience SWV offers better repeatability, voltammograms better resolved and less distorted by capacitive effects, as well as analysis performed at higher speed and less surface poisoning [18,32].

An important parameter for the interaction is the duration of incubation. The optimal incubation time was investigated with biosensor immersed in the 2.0 × 10^{-4} M PG solution for different incubation time ranged from 10 to 60 min. The decrease of dA peak current was followed and presented as normalized values in the Table S2 in the Supplementary Material. The lowest value, i.e. the most pronounced dA peak intensity decrease, was obtained for 30 min of interaction. Therefore 30 min was adopted for further work as optimal interaction time for ADs with DNA, what is in accordance with time previously determined for precursor substance 9-chloroacridine [18,42].

When biosensor was incubated in the solution containing 2.4 × 10^{-4} M AD in acetate buffer pH 4.6, *I* 0.1 M for 30 min, a significant decrease in the current of dA peak was observed (Fig. 2, curve 3) indicating possible interaction. It may be assumed that AD – DNA interaction was accompanied with a decrease in the ability of adenosine moieties to be oxidized, probably by being shield with the AD molecules. No changes in dA peak height were observed when DNA sensor was incubated in blank acetate buffer pH 4.6, *I* 0.1 M for 30 min without the addition of

acridines.

On the other hand, after the interaction, at the potential about + 1.0 V the current of the peak denoted as (dG + $I_{interact}$) distinctly increased. The obtained signal consisted of the current contributions from oxidation of both deoxyguanosine and AD electroactive species, and therefore its change was not informative.

As seen in Fig. 2, these observations are true for all four investigated derivatives, being most pronounced in the case of PG and PA.

Along with decrease in dA peak current, a positive shift of 11 mV − 15 mV in dA oxidation peak potential was observed after incubating in ADs solution. The dA peak displacement indicated that an interaction between surface immobilized DNA and acridine derivatives occurred, and the shift in positive direction referred that the type of interaction was most likely an intercalation [18,43].

As confirmed with the control sample, DNA solution contained other DNA fragments beside dsDNA, therefore the partial intercalation model of compound binding to DNA by stacking between two adjacent bases on the same strand of the DNA, can also be applied [44,45]. The scale of interaction can again be presented by normalized dA peak current [18,30,31], using adapted equation (1):

$$d(dA)\% = \frac{I_{p,\,dA}}{I_{p0,\,dA}} \times 100 \quad (2)$$

where $I_{p,\,dA}$ and $I_{p0,\,dA}$ represent dA signals after and before the interaction with AD. Values of normalized peak currents for all ADs at 30 min incubation time obtained by using the equation (2) are shown in the Table 1. As seen, normalized peak current values are between 22 % for PG, and 67 % for EA. Such small value in the case of PG indicated it's most intensive interaction with DNA, comparing to other ADs, as it was indicated in our previous work comparing PG with other synthesized ADs in our laboratory [8,46]. The PA and EG normalized peak current values lie between 32 % and 35 % what is very satisfactory result, comparing to moderate 67 % current change obtained when EA was interacting with DNA.

Multi-layer biosensor was prepared in the way that it was accomplished the spreading of DNA molecules on the surface of the electrode and its complete coverage. That kind of organization was essential to avoid the non-specific adsorption of interacting molecules and biosensor response originated from a compound that is incorporated into the DNA layer, without any contribution from the free compound diffusion from the solution. In another words, after the incubation of DNA (at the electrode surface) with AD in solution for 30 min, and transfer to the blank buffer, the peaks recorded for the oxidation of AD could only be attributed to the molecules that were inside the DNA layer, i.e. the molecules that have interacted with DNA, while other "free" molecules were removed after rinsing with water and therefore could not be detected.

Voltammograms recorded after the incubation and interaction (Fig. 2. (A-D) red curves), showed peaks at 0.4–0.6 V and 1.05 V that completely and partly, respectively, corresponded to the AD imbedded into DNA film. A broad peak between 0.4 V and 0.6 V (peak II) recorded after the interaction between AD and DNA was present only when the potential was scanned from negative potential limit of −1.4 V, and it was absent when the scan started from zero potential. It can further be suggested that peak II occurred as a signal due to the oxidation of reduction product of AD, formed at the GCE surface inside the DNA layer. The same peak was detected in the CV (Fig. 1, Fig. S2, Fig. S3 and Fig. S4), as well as in SW voltammograms (scanned from negative potential limit of −1.4 V) of ADs recorded from the solution (black lines, Fig. 2.).

On the other hand, these results also indicated that the peak in question couldn't be the consequence of 8-oxo-dG or 2,8-DHA formation which cause the oxidative damage to the guanine or adenine residues [15,47–49] under applied experimental conditions. The fact that supports this assertion is that the oxidative damage is followed up with the increase in both dG and dA peak currents as a consequence of the unwinding of the DNA double helix and greater exposure of guanine and adenine residues to the surface of the electrode. In case of investigated ADs, the height of the dA peak decreased markedly after the exposure to synthesized acridines. All of the above confirm that peak present in the potential range from 0.4 to 0.6 V does not originate from mutagenic 8-oxo-dG or 2,8-DHA, and none of the synthesized acridine derivatives do not promote oxidative damage to DNA through the generation of these reactive oxygen species.

As mentioned earlier, after the interaction instead of separate dG and I peaks, only one peak at around 1.04 V occurred, with distinctly increased peak current. This peak was denoted as (dG + $I_{interact}$) since it consisted of the current contributions from oxidation of both electroactive species (deoxyguanosine and certain acridine derivative inside the DNA layer) at the electrode surface. According to the results, there was no correlation between the exact increase of the current and the amount of AD in the incubation solution. Such behaviour was probably due to the fact that their individual peak potentials were considerably different and therefore these electroactive species participated with different contributions to the recorded current. Therefore, due to the overlapping of those two peaks the results were not informative.

The increased current at 1.04 V confirmed the interaction during which AD molecules were brought closer to the electrode surface as they were captured in the DNA network, what allowed them easier electron exchange. Unfortunately, this phenomenon precluded quantitative consideration of the (dG + $I_{interact}$) peak current as previously pointed out, and for all further considerations of the interaction, only dA peak height and position were used.

3.3. Acridine derivatives concentration profiles obtained by SWV using DNA/GCE

The DNA electrochemical biosensor was used to investigate the concentration profile of synthesized ADs and to determine the lowest detectable content able to interact with DNA. For that purpose, a wide concentration range of ADs was investigated (Fig. 4) by measuring the change in the intensity of the dA peak which is the only peak informative in voltammograms obtained with DNA/GCE sensor incubated in ADs solutions (as explained previously).

Among all investigated ADs, PG showed the widest range of concentration capable to interact with DNA. The decrease in dA peak current was detected when PG was present in the solution in the concentration ranged from 1×10^{-7} M to 2.5×10^{-4} M (Fig. 4A). For each concentration, fresh DNA electrochemical biosensor was prepared and immersed in acetate buffer pH 4.6, *I* 0.1 M, with different PG concentration, for 30 min. SW voltammograms were taken after the transfer of the electrode into the blank, deaerated, background electrolyte. To be sure, that SW peak at + 1.3 V originated entirely from the deoxyadenosine moieties oxidation (dA peak), the control measurement was done when the bare GCE (instead of DNA biosensor) was immersed for 30 min in the PG solution of the highest concentration, under the same experimental conditions. As seen at Fig. 4A curve 17, no signal from PG was detected. The same situation was observed with other three ADs (Fig. 4 B-D, curve 11).

With the increasing of PG concentration, the decrease in dA peak was evident, while the peak potential moved to more positive values. The dA peak current decreased rapidly with low PG contents and when the concentration reached level of 10^{-5} M it started to level off. The current changes of deoxyadenosine peak dA in relation to the PG concentration is shown at the Fig. 5. Three areas were distinguished, the first two: I (1×10^{-7} M − 9×10^{-7} M) and II (1×10^{-6} M − 5×10^{-6} M) showed linear relationship with different slopes, and the third one ($c > 5 \times 10^{-6}$ M) showed the current levelling off with the increase of PG concentration. The characteristics of linear plots for first two concentration regions are summarized in Table 2. The limit of detection (LOD) and limit of quantification (LOQ) for PG quantification with DNA modified GCE following the SW voltammetric measurement procedure were calculated

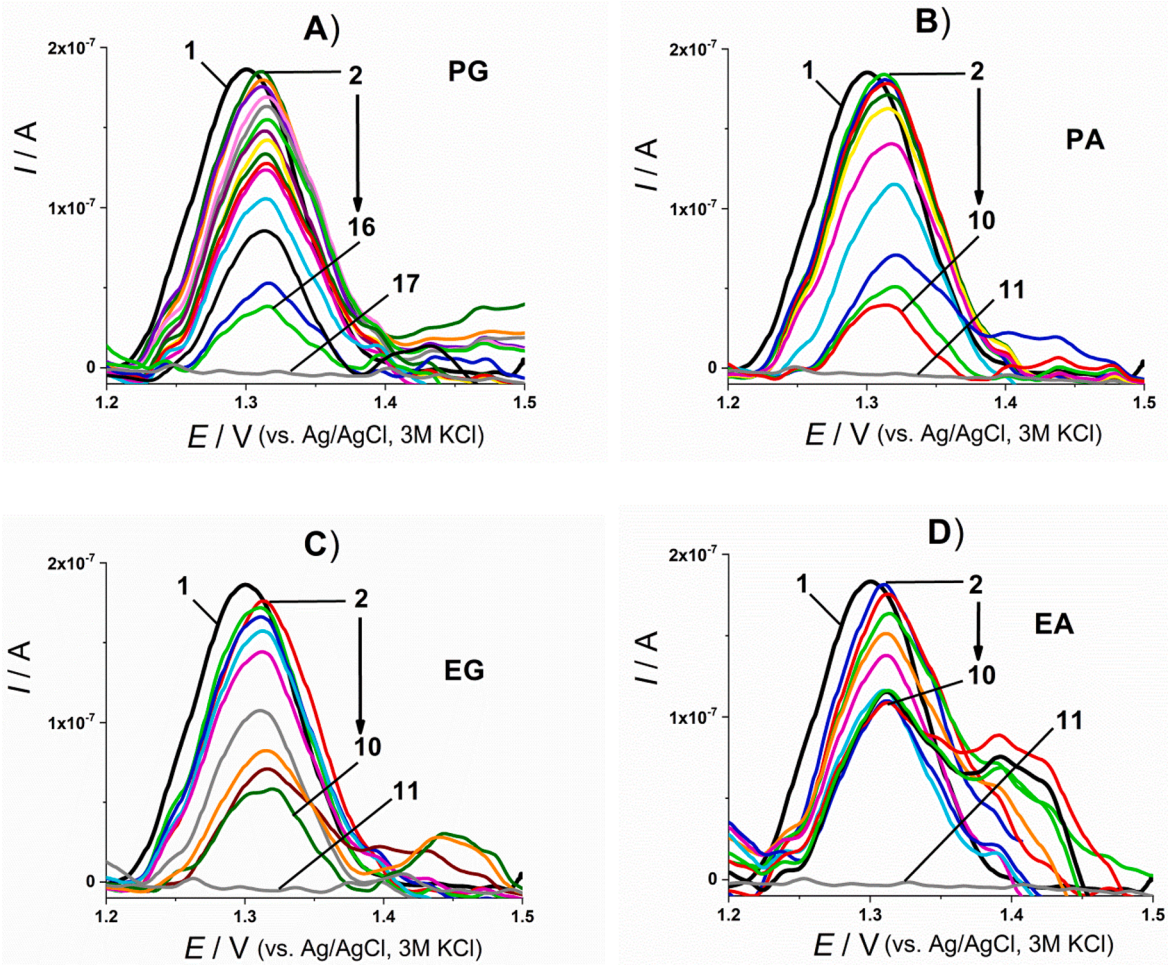

Fig. 4. Corrected SW voltammograms of DNA biosensor after interaction with different concentration of acridine derivatives: A) PG; B) PA; C) EG and D) EA. **A** 1) DNA biosensor 2) 1×10^{-7} M 3) 3×10^{-7} 4) 4.5×10^{-7} 5) 5.6×10^{-7} 6) 6.2×10^{-7} 7) 9.2×10^{-7} 8) 1.9×10^{-6} 9) 3.1×10^{-6} 10) 4.4×10^{-6} 11) 5.3×10^{-6} 12) 10×10^{-6} 13) 2.5×10^{-5} 14) 6.5×10^{-5} 15) 1.00×10^{-4} 16) 2.50×10^{-4} M 17) SW voltammogram recorded after 30 min incubation of bare GCE in 2.4×10^{-4} M PG solution **B** 1) DNA biosensor 2) 6×10^{-7} M 3) 7.5×10^{-7} 4) 1×10^{-6} 5) 1.8×10^{-6} 6) 3.7×10^{-6} 7) 7.5×10^{-6} 8) 5.0×10^{-5} 9) 1.00×10^{-4} 10) 2.4×10^{-4} M 11) SW voltammogram recorded after 30 min incubation of bare GCE in 2.4×10^{-4} M PA solution **C** 1) DNA biosensor 2) 2×10^{-7} M 3) 4×10^{-7} 4) 1.6×10^{-6} 5) 5.7×10^{-6} 6) 8.0×10^{-6} 7) 2.0×10^{-5} 8) 5.0×10^{-5} 9) 1.00×10^{-4} 10) 2.4×10^{-4} M 11) SW voltammogram recorded after 30 min incubation of bare GCE in 2.4×10^{-4} M EG solution **D** 1) DNA biosensor 2) 1×10^{-5} M 3) 1.5×10^{-5} 4) 3.4×10^{-5} 5) 4.5×10^{-5} 6) 6.8×10^{-5} 7) 3.40×10^{-4} 8) 4.80×10^{-4} 9) 1.00×10^{-4} 10) 2.4×10^{-4} M 11) SW voltammogram recorded after 30 min incubation of bare GCE in 2.4×10^{-4} M EG solution.

using the equations LOD $= \frac{3S_a}{b}$ and LOQ $= \frac{10S_a}{b}$ where S_a represents the standard deviation of the intercept, and b is the slope of the regression curve. Statistical parameters of the regression lines are given in Table 2.

Using the above equations, the obtained LOD and LOQ values for I linear concentration range of PG were 5.39×10^{-8} M and 1.80×10^{-7} M, respectively. Such low PG concentrations that have been proven to interact with DNA, confirm its strong binding ability towards DNA. It should be pointed out that these two linear concentration regions have quite different slopes, indicating different affinity towards DNA layer. The slope of segment I is almost six times higher compared to segment II, what, among other things has direct impact on LOD and LOQ values. Therefore, in linear concentration range II (1×10^{-6} M $- 5 \times 10^{-6}$ M) values for LOD $= 3.75 \times 10^{-7}$ M, and LOQ $= 1.25 \times 10^{-6}$ M were obtained.

Synthesized acridine derivatives PA and EG showed resembling concentration profiles. The rapid decrease of the dA current was observed for EG concentration in the range 2×10^{-7} M $- 8 \times 10^{-6}$ M and was followed by a levelling off at concentrations higher than 1×10^{-5} M (Fig. 4C). In the case of PA (Fig. 4B), slightly higher initial concentration caused a detectable change in dA peak intensity, but the levelling off was again recorded at concentrations over 1×10^{-5} M (Table 2.). The slope values were similar for both ADs, amounted about 0.004 A M^{-1} and the corresponding LOD values were 4.27×10^{-7} M for EG and 7.03×10^{-7} M in the case of PA. Concentration profiles for these derivatives are shown in Supplementary Material, Fig. S5 and Fig. S6.

Research done with derivative EA showed that markedly higher concentrations were needed to manifest the interaction with DNA, compared to previously mentioned compounds (Fig. 4D). The linear decrease of dA peak current was recorded with concentrations which previously caused the levelling off, i.e. in the range between 1×10^{-5} – 1×10^{-4} M, but with ten times less steep slope. Consequently, the LOD and LOQ values were higher, being 7.26×10^{-6} M and 2.42×10^{-5} M, respectively. Above the EA concentration of 1×10^{-4} M, a loss of linearity was observed (Fig. S7). The characteristics of this regression plot are also summarized in the Table2.

The main goal of this investigation was to find the concentration profile of synthesized ADs and to determine the lowest detectable content able to interact with DNA. According to obtained results, the best response was observed with PG indicating the best interaction capability. Also, both the LOD and LOQ values confirmed the sensitivity of the measured results.

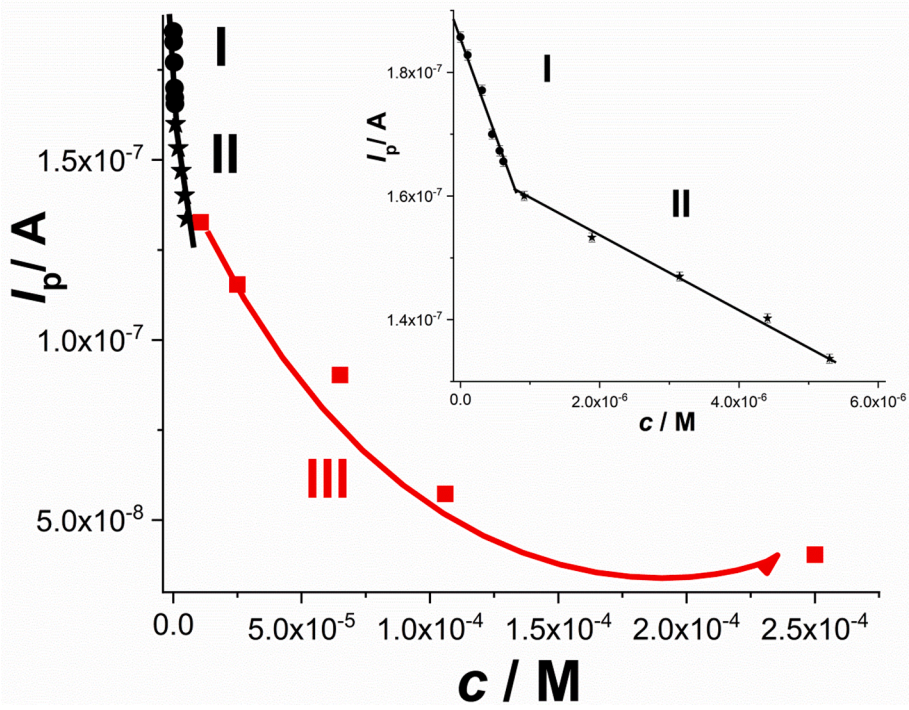

Fig. 5. Dependence of SWV dA peak current, on the concentration of PG incubation solutions. Inset: Ranges of linear dA peak current decrease for: concentration range I: 1×10^{-7} M – 9×10^{-7} M, y = -0.033 × + 1.86×10^{-7}; $R^2 = 0.989$; concentration range II: 1×10^{-6} M – 5×10^{-6} M, y = -0.0058 × + 1.65×10^{-7}; $R^2 = 0.994$.

Table 2
Basic statistic data of the regression lines for quantification of PG, EG, PA and EA at DNA/GCE by SWV.

Data	Acridine derivatives, AD			
	PG	EG	PA	EA
Linear range (M)	1×10^{-7} – 9×10^{-7} (I) 1×10^{-6} – 5×10^{-6} (II)	2×10^{-7} – 8×10^{-6}	6×10^{-7}–7.5×10^{-6}	1×10^{-5} – 1×10^{-4}
Regression equation y = *I* (A); x = *c* (M)	y = –0.033x +1.86×10^{-7} (I) y= –0.0058x+1.65×10^{-7} (II)	y = –0.0039x + 1.81×10^{-7}	y = –0.0047 x + 1.86×10^{-7}	y = – 0.00065 x + 1.85×10^{-7}
Number of points	6 (I) 5 (II)	8	7	7
Slope (AM^{-1})	–0.03345 (I) –0.0058 (II)	–0.00392	–0.00474	–0.000653
Intercept (A)	1.86162×10^{-7} (I) 1.65013×10^{-7} (II)	1.80954×10^{-7}	1.86414×10^{-7}	1.84681×10^{-7}
Correlation coefficient	– 0.9962 (I) – 0.9981 (II)	–0.9959	–0.9872	–0.9885
S.D. of slope ($A\ M^{-1}$)	1.46×10^{-3} (I) 2.06×10^{-4} (II)	1.46×10^{-4}	3.42×10^{-4}	4.99×10^{-5}
S.D. of intercept (A)	6.01×10^{-10} (I) 7.25×10^{-10} (II)	5.58×10^{-10}	1.11×10^{-9}	1.58×10^{-9}
SD (A)	8.18×10^{-10} (I) 7.37×10^{-10} (II)	1.11×10^{-9}	2.18×10^{-9}	2.25×10^{-9}
LOD (M)	5.39×10^{-8} (I) 3.75×10^{-7} (II)	4.27×10^{-7}	7.03×10^{-7}	7.26×10^{-6}
LOQ (M)	1.80×10^{-7} (I) 1.25×10^{-6} (II)	1.42×10^{-6}	2.34×10^{-6}	2.42×10^{-5}

3.4. Evaluation of acridine derivatives – DNA binding constants

It may be assumed that during the interaction between AD in the solution and DNA molecules adsorbed on the electrode surface the complex has been formed. Concentration of DNA adsorbed on the electrode surface was constant whilst AD concentration increased during experiment. To evaluate the composition of the association complexes and binding constants for the formation of AD–DNA complex, the conventional equilibrium reaction for an association was employed:

$DNA_{ads} + n(AD) \leftrightarrow (AD)_n\text{–}DNA_{ads}$.

where the individual components equilibrium concentrations are considered as a part of the total concentration in the reaction mixture: $[DNA_{ads}] = c(DNA_{ads}) - [(AD)_n\text{-}DNA_{ads}]$ and $[AD] = c(AD) - [(AD)_n\text{-}DNA_{ads}]$.

To analyze the formed supramolecular compound in the adsorbed state, and to determine the apparent binding constant, the modification of standard titration procedure [32] was used and corresponding equilibrium constant (*K*) is given by the equation:

$$K = \frac{[(AD)_n - DNA_{ads}]}{[DNA_{ads}][AD]^n} \quad (3)$$

with n representing the molar relation of AD that interacts with a molar quantity of DNA bases [50].

After the transformation of the previous expression, the following equation is obtained

$$\log\left[\frac{I_{complex}}{I_{DNA} - I_{complex}}\right] = -n\log K - n\log c_{AD} \quad (4)$$

where I_{DNA} and $I_{complex}$ represent dA peak currents in the absence of AD and with different AD concentrations forming AD-DNA complex, respectively. According to equation (4) the values for binding constant of the adsorbed complexes could be determined, based on the obtained values for slope ($-n$) and intercept ($-n\log K$) of the linear dependence $\log\left[\frac{I_{complex}}{I_{DNA}-I_{complex}}\right]$ *vs* $\log c_{AD}$. In the case of PG, an acridine derivative that interacts with DNA in the widest concentration range, three areas of linearity with different slopes were observed. The fact that there are different slopes in the plot confirms more than a single complex formation [51].

As shown at Fig. 6., linear range I that correspond to lowest PG concentrations, display the slope of $n = 1.053$ indicating the 1: 1 association complex, and combined with intercept gives the value of binding constant equal to 8.68×10^5 M^{-1}. This value, close to the 10^6 M^{-1} refers to strong binding. With increased concentration of PG in the incubation solution, the slope of $\log\left[\frac{I_{complex}}{I_{DNA}-I_{complex}}\right]$ *vs* $\log c_{PG}$ dependence in linear range II decreased to $n = 0.485$ ($n \approx 0.5$) indicating the 1: 2 association complex, and correspondingly the reduced binding constant value of 2.31×10^4 M^{-1} was obtained. In third linear range (III), the slope was again close to unity ($n = 0.804$), but the corresponding binding constant was even smaller $K = 2.05 \times 10^4$ M^{-1}. These results, which are systematized in Table 3, indicated that PG form stable complexes with DNA, but their binding characteristics change with concentration of PG. It seems that low concentrations of PG are favourable attached to DNA network under these conditions. Probably the change in DNA layer morphology caused by PG insertion was thermodynamically most favourable at low concentration (as indicated by the obtained ΔG value). The decrease in K with the increase of PG concentration may be caused by the change in orientation, possible repulsion, previously blocked DNA bases, or other processes that make the bases less accessible for interaction.

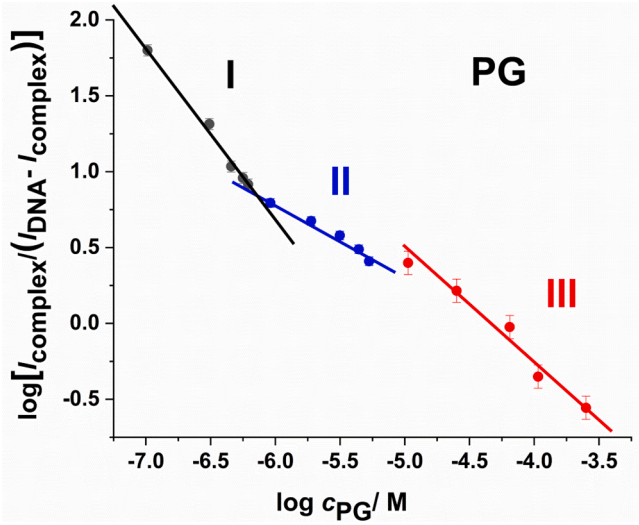

Fig. 6. Dependence of $\log\left[\frac{I_{complex}}{I_{DNA}-I_{complex}}\right]$ *vs* $\log c_{PG}$ used for PG-DNA binding constant determination. I: y = -1.053 × − 6.253; $R^2 = 0.989$. II: y = -0.485 × − 2.117; $R^2 = 0.974$. III: y = -0.804 × − 3.467 × 10^{-7}; $R^2 = 0.967$.

Compound PA showed two linear regions with slopes of $n \approx 1$ and $n \approx 0.5$ (Fig. 7.), and corresponding binding constants of $K = 2.80 \times 10^4$ M^{-1} and $K = 4.57 \times 10^4$ M^{-1}, respectively. The obtained binding constants were less compared to PG, what is in accordance with concentration able to interact. Again, two types of complexes were obtained (Table 3). The values of PA-DNA binding constants may be classified as medium strength.

Compounds EG and EA showed low K values, 7.59×10^3 M^{-1} and 5.67×10^3 M^{-1}, respectively. These values were lower than average compared to the reported values for other compounds and drugs that interact with DNA (Table 4) and values obtained for PA and particularly PG. Based on the slopes of the given dependencies being −0.59, and −1.11 for EG and EA, respectively (Fig. 8A and Fig. 8B) it may be concluded that the composition of the formed adsorbed association complexes was 1: 2 in the case of EG and 1: 1 in the case of EA. In both cases, higher AD concentrations showed the investigated logarithmic dependence levelling-off, with slope $n < 0.1$. Such low values of the slope indicated the complete coverage of DNA layer with AD molecules.

In most of the available literature data, the 1: 1 association complex is typically reported and considered [52,53]. Our results unequivocally show that association complex may vary depending on the concentration of the interacting substance. Also the difference in the molar relation of AD that interacts with a molar quantity of DNA bases may be the consequence of the presence of other segments of DNA different from dsDNA, i.e. the occurrences of partial intercalation model of binding to DNA by stacking between two adjacent bases on the same strand of the DNA.

To our best knowledge small molecule-DNA interaction was newer investigated in such wide concentration range, also association complex different from 1: 1 for acridine derivatives - DNA complexes is reported for the first time.

According to literature, intercalation-based interactions are characterized with high K values usually 10^4 – 10^6 M^{-1}, while the lower K values implied a rather weaker interaction such as groove or electrostatic [53]. Some examples are listed in Table 4.

To obtain the cognition whether the interaction processes between ADs and DNA are thermodynamically favourable, the change in the Gibbs free energy (ΔG) was calculated using the well-known equation $\Delta G = -RT\ln K$ [38]. The results obtained for all investigated derivatives using the calculated binding constants at room temperature 25 °C are presented in Table 3. The negative ΔG value for all ADs was obtained in the range of − 21 to − 34 kJ mol^{-1}, confirming the process spontaneity. The best result, indicating the most stable formed complex with DNA adsorbed at the electrode surface, showed PG when present in low concentration order of 10^{-7} M.

According to the results presented in Table 3 the highest binding constant values and the lowest ΔG values were shown by PG upon interacting with DNA, implying that it builds the most stable complex. Besides PG, derivative PA also forms complexes with $K > 10^4$ M^{-1}, which is considered a measure of fairly strong interaction. Specified data, along with the SW signal shift in the positive direction indicated intercalation as the mode of interaction. Compounds EG and EA demonstrated weaker interaction with DNA what is indicated by both lower values of K ($<10^4$ M^{-1}) and less negative values of ΔG. However, although smaller, a positive shift in peak potential was noticeable with these compounds as well, and therefore it can be assumed that these compounds also intercalated into a DNA helix. Considering slightly lower K values the existence of groove binding cannot be excluded [53]. Differences in type of interaction arise as a consequence of different ADs reacting concentrations, as well as the probable modifications in the morphological conformation of DNA helix upon binding [53].

3.5. Molecular docking

Acridine derivatives intercalate into DNA and act as topoisomerase II poisons [63]. In our previous study, topoisomerase II inhibitory

Table 3
Values of AD - DNA binding constants, the molar relation of AD that interacts with a molar quantity of DNA bases and Gibbs free energy change.

Acridine derivative	Concentration range (M)	SD*	K (M^{-1})	n	Association complex	ΔG kJ mol^{-1}
PG	1×10^{-7}–9×10^{-7}	0.036	8.68×10^{5}	1.053	1:1	–33.90
	1×10^{-6}–5×10^{-6}	0.028	2.31×10^{4}	0.485	1:2	–24.91
	1×10^{-5}–2.5×10^{-4}	0.076	2.05×10^{4}	0.804	1:1	–24.61
PA	6×10^{-7}–1×10^{-5}	0.093	2.80×10^{4}	1.035	1:1	–25.38
	5×10^{-5}–2.5×10^{-4}	0.043	4.57×10^{4}	0.469	1:2	–26.60
EG	2×10^{-7}–8×10^{-6}	0.075	7.59×10^{3}	0.595	1:2	–22.15
	1×10^{-5}–2.5×10^{-4}		/	/	/	/
EA	1×10^{-5}–1×10^{-4}	0.084	5.67×10^{3}	1.109	1:1	–21.42
	1×10^{-4}–5×10^{-4}		/	/	/	/

* SD – Standard deviation of the of the regression line's: $\log\left[\frac{I_{complex}}{I_{DNA} - I_{complex}}\right]$ *vs* $\log c_{AD}$ i.e. the standard deviation of the residuals.

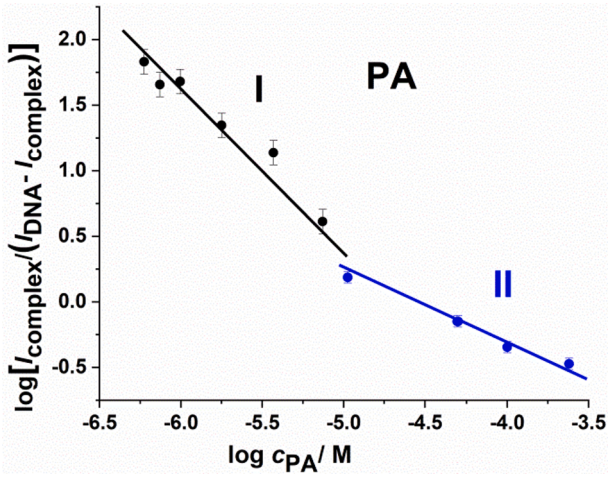

Fig. 7. Dependence of $\log\left[\frac{I_{complex}}{I_{DNA} - I_{complex}}\right]$ *vs* $\log c_{PA}$ used for PA-DNA binding constant determination. I: y = -1.035 × − 4.604; R^2 = 0.966. II: y = -0.469 × − 2.186; R^2 = 0.965.

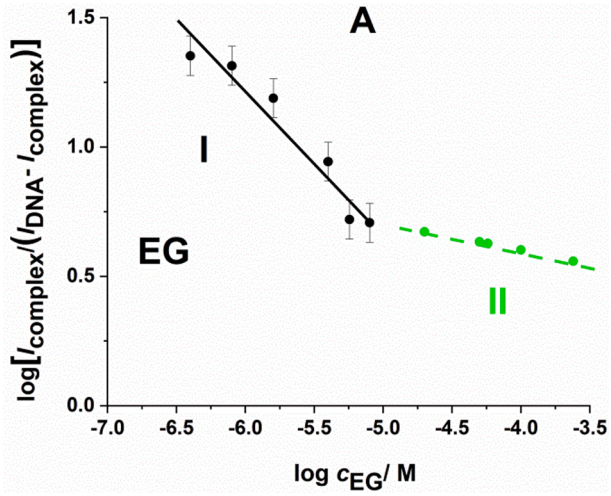

Fig. 8A. Dependence of $\log\left[\frac{I_{complex}}{I_{DNA} - I_{complex}}\right]$ *vs* $\log c_{EG}$ used for EG-DNA binding constant determination. I: y = -0.595 × − 2.310; R^2 = 0.959. II: slope ≈ 0.

Table 4
Binding constants and proposed binding mode of some drugs /compounds interacting with DNA.

Drug / compound	Binding constant (M^{-1})	Binding mode	Reference
Daunomicin	7.0×10^{5}	intercalation	[54]
Oseltamivir	1.8×10^{4}	intercalation	[55]
Rifampicin	5.2×10^{5}	intercalation	[56]
Ribavirin	4.3×10^{3}	groove binding	[57]
Rosiglitazone	3.4×10^{3}	groove binding	[58]
Tenofovir	6.8×10^{6}	intercalation	[59]
Acridine orange	2.7×10^{4}	intercalation	[60]
Metilen blue	1.2×10^{4}	intercalation	[61]
Quercetin	4.8×10^{3}	groove binding	[62]
9Cl-Acridine	3.4×10^{5}	intercalation	[18]

potential of compounds PG, PA, EG and EA was proved and it was similar to amsacrine [8]. In this study, binding of compounds PG, PA, EG and EA to the DNA/topoisomerase II complex was investigated in silico. Docking was performed on chain B of topoisomerase II and only part of DNA surrounding the binding site was retained. All tested compounds had slightly higher binding energies (from − 8.6 to − 8.9 kcal mol^{-1}) in comparison to amsacrine (− 10.1 kcal mol^{-1}). In comparison to amsacrine, PG, PA and EA were similarly orientated in the receptor site. The most significant interactions of compound PG with DNA were between acridine ring and DA12, DT9 (π-π stacked) and DC8 (π-alkyl). Acridine ring of compound EA formed interactions with DA12 and DC8 (π-π stacked), while its amino group formed hydrogen bond interaction with

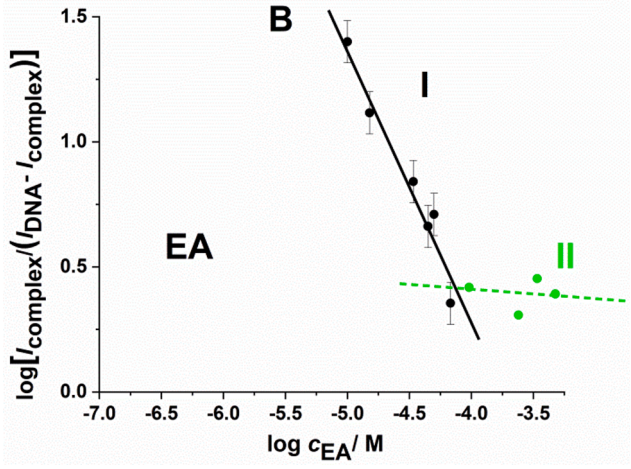

Fig. 8B. Dependence of $\log\left[\frac{I_{complex}}{I_{DNA} - I_{complex}}\right]$ *vs* $\log c_{EA}$ used for EA-DNA binding constant determination. I: y = -1.109 × − 4.163; R^2 = 0.957. II: no linearity.

DT9. Acridine ring of compound PA formed interactions with DA12, DT9 and DC8 (π-π stacked). Compound EG was differently orientated in the receptor site, but its acridine ring formed π-π stacked interactions with DA12, DC8 and DT9. According to these results, compounds PG, PA, EG and EA have potential to interact with DNA and act as DNA intercalators

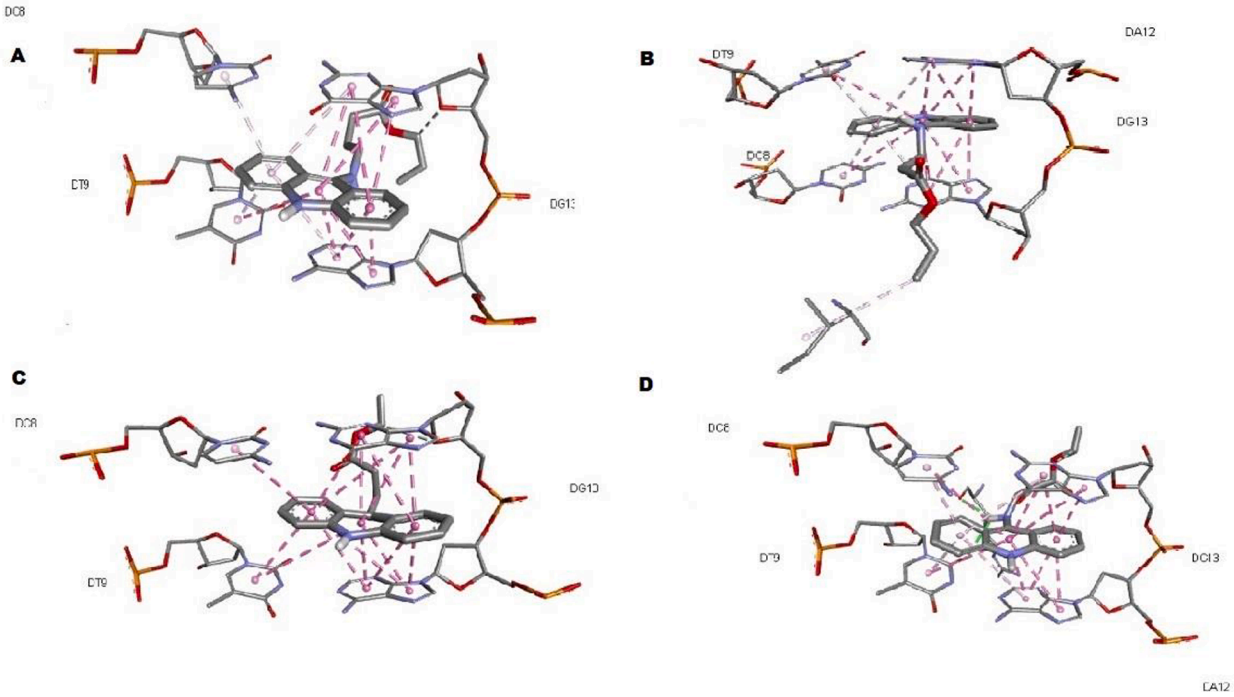

Fig. 9. Binding of PG (A), PA (B), EG (C) and EA (D) to DNA/topoisomerase II complex.

(Fig. 9).

4. Conclusions

The most potent previously synthesized anticancer candidates, 9-acridinyl amino acid derivatives PG, PA, EG, and EA, were selected and investigated by applying SWV using a GCE. Oxidation, studied in acetate buffer at pH 4.6, revealed two irreversible SWV peaks. All four ADs showed very modest adsorption (d(I) ≈ 3 – 15 %) at bare GCE after 30 min incubation at OCP (open circuit potential). On the other hand, when incubation was performed with DNA-biosensor where the complete coverage was accomplished, AD's characteristic peaks originated entirely from molecules that were incorporated into the DNA layer appeared quite pronounced.

The DNA multi-layer electrochemical biosensor was used to confirm and characterize the interaction between PG, PA, EG or EA and surface immobilized DNA by the change in dA oxidation peak position and decrease of its peak current after a 30 min of incubation.

The PG showed the widest range of concentration capable to interact with DNA (1×10^{-7} M to 2.5×10^{-4} M) and extreme low LOD (5.39×10^{-8} M). Three areas in concentration profile of PG interacting with DNA were present, indicating different strength of interaction. The situation was similar with the other ADs, but they haven't shown more than two areas of concentration which were in narrower range and generally with higher LOD values. Compared to others, EA showed markedly higher concentrations needed to manifest the interaction with DNA. Results indicated that investigated compounds did not cause the oxidative damage to DNA, since mutagenic 8-oxoG residue was not detected under applied experimental conditions.

When present in low concentration order of 10^{-7} M, PG showed the highest value of binding constant ($K = 8.68 \times 10^5$ M^{-1}), indicating the most stable complex formed with DNA which was adsorbed at the electrode surface. With the increase in PG concentration the binding constants decreased (2.31×10^4 M^{-1} and 2.05×10^4 M^{-1}). Compound PA also formed complexes with $K > 10^4$ M^{-1}, which was considered as a measure of fairly strong interaction, while EG and EA demonstrated weaker interaction with DNA ($K < 10^4$ M^{-1}). It was shown that the binding characteristics of the association AD–DNA complex changed with the concentration of interacting compound in the incubating solution, and the presence of other DNA fragments beside dsDNA. The negative ΔG values obtained with all ADs, confirmed the spontaneity of the binding processes. The binding was thermodynamically less favourable for higher ADs concentrations, probably due to the successive blocking of DNA bases with increasing AD concentration, and change in DNA layer morphology upon binding.

The decrease in current intensity, along with the SW signals shift in the positive direction indicated intercalation as the mode of interaction of all four compounds with DNA. Considering the slightly lower K values, besides intercalation as a dominant mode, the existence of groove binding couldn't be excluded for EG and EA.

The intercalation into DNA was supported by molecular docking analysis, which showed that compounds PG, PA, EG and EA have potential to interact with DNA and act as DNA intercalators.

The novelty of this study is in providing insight into oxidation processes and the effect of ADs concentration on the type and mechanism of AD-DNA interaction. It also promotes PG, among the other three compounds, as the best anticancer candidate for further research. The use of DNA biosensors in the screening of the compounds with potential anticancer activity proved to be very useful for new antineoplastic drugs development due to its low cost, great speed and simplicity.

In addition to contributing in understanding the mechanism of interaction, such an approach simulates *in vivo* contact thus avoiding expensive and complicated experiments for the initial testing of anticancer candidates.

Declaration of Competing Interest

The authors declare that they have no known competing financial interests or personal relationships that could have appeared to influence the work reported in this paper.

Data availability

No data was used for the research described in the article.

Acknowledgements

This research was funded by the Ministry of Education, Science and Technological Development, Republic of Serbia through Grant Agreement with University of Belgrade-Faculty of Pharmacy No: 451-03-68/2022-14/200161. The authors are grateful to Dr. Miljana Tanić for her help with fluorimetric and electrophoresis measurements.

Appendix A. Supplementary data

Supplementary data to this article can be found online at https://doi.org/10.1016/j.bioelechem.2022.108323.

References

[1] J. Rupar, V. Dobričić, M. Aleksić, J. Brborić, O. Čudina, A review of published data on acridine derivatives with different biological activities, Kragujevac Journal of, Science 40 (2018) 83–101, https://doi.org/10.5937/KgJSci1840083R.
[2] J. Joseph, E. Kuruvilla, A.T. Achuthan, D. Ramaiah, G.B. Schuster, Tuning of intercalation and electron-transfer processes between DNA and acridinium derivatives through steric effects, Bioconjug. Chem. 15 (2004) 1230–1235, https://doi.org/10.1021/bc0498222.
[3] S.C. Oliveira, A.M. Oliveira-Brett, DNA-Electrochemical Biosensors: AFM Surface Characterisation and Application to Detection of In Situ Oxidative Damage to DNA, Comb. Chem. High Throughput Screen. 13 (2010) 628–640, https://doi.org/10.2174/138620731100407062 8.
[4] P. Singh, A. Kumar, A. Sharma, G. Kaur, Identification of amino acid appended acridines as potential leads to anti-cancer drugs, Bioorganic & Medicinal Chemistry Letters 25 (2015) 3854–3858, https://doi.org/10.1016/j.bmcl.2015.07.059.
[5] C. Gao, F. Liu, X. Luan, C. Tan, H. Liu, Y. Xie, Y. Jin, Y. Jiang, Novel synthetic 2-amino-10(3,5-dimethoxy)benzyl-9(10H)-acridinone derivatives as potent DNA-binding antiproliferative agents, Bioorg. Med. Chem. 18 (2010) 7507–7514, https://doi.org/10.1016/j.bmc.2010.08.058.
[6] Y. Wang, D. Gao, B. Chu, C. Gao, D. Cao, H. Liu, Y. Jiang, Exposure of CCRF-CEM cells to acridone derivative 8a triggers tumor death via multiple mechanisms, Proteomics 16 (2016) 1177–1190, https://doi.org/10.1002/pmic.201500317.
[7] S.A. Lyakhov, I.Y. Suveyzdis, O.V. Bykhovskaya, N.M. Isko, S.A. Andronati, L. A. Litvinova, Biological Acitve Acridine Derivatives. Part 3. Acridinylamino Acids and Their Esters: Synthesis and Cytostatic Activity, Pharmazie. 52 (1997) 560–562, https://doi.org/10.1002/chin.199746202.
[8] J. Rupar, V. Dobričić, J. Grahovac, S. Radulović, Ž. Skok, J. Ilaš, M. Aleksić, J. Brborić, O. Čudina, Synthesis and evaluation of anticancer activity of new 9-acridinyl amino acid derivatives, RSC Med. Chem. 11 (2020) 378–386, https://doi.org/10.1039/c9md00597h.
[9] M. Aslanoglu, Electrochemical and spectroscopic studies of the interaction of proflavine with DNA, Anal. Sci. 22 (2006) 439–443, https://doi.org/10.2116/analsci.22.439.
[10] A.M. Oliveira Brett, V.C. Diculescu, A.M. Chiorcea-Paquim, S.H.P. Serrano, Chapter 20 DNA-electrochemical biosensors for investigating DNA damage, Compr. Anal. Chem. 49 (2007) 413–437. https://doi.org/10.1016/S0166-526X(06)49020-6.
[11] V.C. Diculescu, A.M. Chiorcea-Paquim, A.M. Oliveira-Brett, Applications of a DNA-electrochemical biosensor, Trends Anal. Chem. 79 (2016) 23–36, https://doi.org/10.1016/j.trac.2016.01.019.
[12] E.E.S. Bruzaca, I.C. Lopes, E.H.C. Silva, P.A.V. Carvalho, A.A. Tanaka, Electrochemical oxidation of the antitumor antibiotic mitomycin C and in situ evaluation of its interaction with DNA using a DNA-electrochemical biosensor, Microchemical Journal 133 (2017) 81–89, https://doi.org/10.1016/j.microc.2017.03.030.
[13] W.B.S. Machini, I.P.G. Fernandes, A.M. Oliveira-Brett, Antidiabetic Drug Metformin Oxidation and in situ Interaction with dsDNA Using a dsDNA-electrochemical Biosensor, Electroanalysis 31 (2019) 1–12, https://doi.org/10.1002/elan.201900162.
[14] B. Dogan-Topal, S.A. Ozkan, B. Uslu, The Analytical Applications of Square Wave Voltammetry on Pharmaceutical Analysis, Open Chem. Biomed. Methods J. 3 (2010) 56–73. https://doi.org/10.2174/1875038901003010056.
[15] A.-M. Chiorcea-Paquim, A.M. Oliveira-Brett, DNA Electrochemical Biosensors for In Situ Probing of Pharmaceutical Drug Oxidative DNA Damage, Sensors. 21 (2021) 1125, https://doi.org/10.3390/s21041125.
[16] B. Dogan-Topal, B. Bozal-Palabiyik, S.A. Ozkan, B. Uslu, Investigation of anticancer drug lapatinib and its interaction with dsDNA by electrochemical and spectroscopic techniques, Sens. Actuators, B. 194 (2014) 185–194, https://doi.org/10.1016/j.snb.2013.12.088.
[17] R.R. Deepa, A.A.D. Arulraj, A.K.A.S. Mideen, R.R. Gandhidasan, V.S. Vasantha, Evaluation of Antioxidant Property of Quinones and Calculation of their Binding Constant Values with DNA by Electrochemical Technique, Der Pharma Chem. 10 (2018) 69–78.
[18] J. Rupar, M.M. Aleksić, V. Dobričić, J. Brborić, O. Čudina, An electrochemical study of 9-chloroacridine redox behavior and its interaction with double-stranded DNA, Bioelectrochemistry. 135 (2020), 107579, https://doi.org/10.1016/j.bioelechem.2020.107579.
[19] C.-H. Shen, Chapter 7 – Detection and Analaysis of Nucleic Acids, Diagnostic Molecular Biology, 2019, 167-185. https://doi.org/10.1016/B978-0-12-802823-0.00007-9.
[20] https://www.thermofisher.com/document-connect/document-connect.html?url=https://assets.thermofisher.com/TFS-Assets%2FLSG%2FApplication-Notes%2Fqubit-dsdna-assay-specificity-app-note.pdf , 01. 09. 2022.
[21] D.D. Perrin, B. Dempsey, Buffers of pH and metal ion control, Laboratory Manuals, Chapman and Hall, London, 1974.
[22] O. Trott, A.J. Olson, AutoDock Vina: Improving the Speed and Accuracy of Docking with a New Scoring Function, Efficient Optimization, and Multithreading, J. Comput. Chem. 31 (2010) 455–461, https://doi.org/10.1002/jcc.21334.
[23] M.F. Sanner, Phyton: a programming language for software integration and development, J. Mol. Graph. Model. 17 (1999) 57–61.
[24] C.C. Wu, Y.C. Li, Y.R. Wang, T.K. Li, N.L. Chan, On the structural basis and design guidelines for type II topoisomerase-targeting anticancer drugs, Nucleic Acids Res. 41 (2013) 10630–10640, https://doi.org/10.1093/nar/gkt828.
[25] Discovery Studio Visualizer, Dassault Systemes, (n.d.).
[26] J. Wang, Analytical Electrochemistry, 3rd ed., Wiley-VHC, New Jersey, 2006.
[27] M.A. Arugula, Y. Zhang, A.L. Simonian, Biosensors as 21st century technology for detecting genetically modified organisms in food and feed, Anal. Chem. 86 (2014) 119–129, https://doi.org/10.1021/ac402898j.
[28] Y. Wang, E. Laborda, R.G. Compton, Electrochemical oxidation of nitrite: Kinetic, mechanistic and analytical study by square wave voltammetry, J. Electroanal. Chem. 670 (2012) 56–61, https://doi.org/10.1016/j.jelechem.2012.02.016.
[29] C. Wu, A. Shah, H. Ye, X. Chen, J. Ye, H. Jiang, B. Chen, X. Wang, H. Yan, Droplet electrochemical study of the pH dependent redox behavior of novel ferrocenyl-carborane derivatives and its application in specific cancer cell recognition, Anal. Chim. Acta. 857 (2015) 39–45, https://doi.org/10.1016/j.aca.2014.12.019.
[30] F. Mollarasouli, B. Dogan-Topal, M.G. Caglayan, T. Taskin-Tok, S.A. Ozkan, Electrochemical, spectroscopic, and molecular docking studies of the interaction between the anti-retroviral drug Indinavir and dsDNA, J. Pharm. Anal. 10 (2020) 473–481, https://doi.org/10.1016/j.jpha.2020.08.004.
[31] M.T. Carter, M. Rodriguez, A.J. Bard, Voltammetric Studies of the Interaction of Metal Chelates with DNA. 2. Tris-Chelated Complexes of Cobalt(III) and Iron(II) with 1,10-Phenanthroline and 2,2'-Bipyridine, J. Am. Chem. Soc. 111 (1989) 8901–8911, https://doi.org/10.1021/ja00206a020.
[32] C.M.A. Brett, A.M. Oliveira Brett, Electrochemistry: Principles, Methods, and Applications, 1st ed., Oxford Science University Publications, Oxford, 1993. https://doi.org/10.1016/0013-4686(94)80035-9.
[33] D. Kul, B. Doğan-Topal, S.A. Özkan, B. Uslu, Poly(acridine orange)-modified glassy carbon electrodes: Electrosynthesis, characterisation and sensor application with uric acid, J. Appl. Electrochem. 44 (2014) 831–840, https://doi.org/10.1007/s10800-014-0691-1.
[34] R.N. Adams, Electrochemistry at solid electrodes, Marcel Dekker Inc., New York, 1969.
[35] S.C.B. Oliveira, A.M. Chiorcea-Paquim, S.M. Ribeiro, A.T.P. Melo, M. Vivan, A. M. Oliveira-Brett, In situ electrochemical and AFM study of thalidomide-DNA interaction, Bioelectrochemistry. 76 (2009) 201–207, https://doi.org/10.1016/j.bioelechem.2009.03.003.
[36] P.V.F. Santos, I.C. Lopes, V.C. Diculescu, A.M. Oliveira-Brett, DNA – Cyanobacterial Hepatotoxins Microcystin-LR and Nodularin Interaction: Electrochemical Evaluation, Electroanalaysis 24 (2012) 547–553, https://doi.org/10.1002/elan.201100516.
[37] S. Kurbanoglu, B. Dogan-Topal, L. Hlavata, J. Labuda, S.A. Ozkan, B. Uslu, Electrochemical investigation of an interaction of the antidepressant drug aripiprazole with original and damaged calf thymus dsDNA, Electrochim. Acta. 169 (2015) 233–240, https://doi.org/10.1016/j.electacta.2015.04.087.
[38] A.M. Oliveira-Brett, J.A.P. Piedade, L.A. Silva, V.C. Diculescu, Voltammetric determination of all DNA nucleotides, Anal. Biochem. 332 (2004) 321–329, https://doi.org/10.1016/j.ab.2004.06.021.
[39] R.A. Hutchins, J.M. Crenshaw, D.E. Graves, W.A. Denny, Influence of Substituent Modifications on DNA Binding Energetics of Acridine-Based Anticancer Agents, Biochemistry. 42 (2003) 13754–13761, https://doi.org/10.1021/bi035434w.
[40] A.D.R. Pontinha, S. Sparapani, S. Neidle, A.M. Oliveira-Brett, Triazole-acridine conjugates: Redox mechanisms and in situ electrochemical evaluation of interaction with double-stranded DNA, Bioelectrochemistry. 89 (2013) 50–56, https://doi.org/10.1016/j.bioelechem.2012.08.005.
[41] A.M. Oliveira-Brett, Electrochemistry for probing DNA damage, in: C.A. Grimes, E. C. Dickey, M.V. Pishko (Eds.), Encycl, American Scientific Publishers, USA, Sensors, 2006, pp. 301–314.
[42] J. Pantić, M.M. Aleksić, V. Dobričić, O. Čudina, J. Brborić, S. Vladimirov, Electrochemical oxidation and interaction of 9-chloroacridine with DNA at glassy carbon electrode, in: 13th Int. Conf. Fundam. Appl. Asp. Phys. Chem. B. Proc., Belgrade, 2016: pp. 383–386.
[43] V. Vyskočil, M. Blašková, A. Hájková, E. Horáková, Z. Krejčová, K. Stávková, J. Wang, Electrochemical DNA biosensors – useful diagnostic tools for the detection of damage to DNA caused by organic xenobiotics (A Review), Sens. Electroanal. 7 (2012) 141–162.
[44] H.S. Rye, A.N. Glazer, Interaction of dimeric intercalating dyes with single-stranded DNA, Nucleic Acids Research 23 (1995) 1215–1222.
[45] N.J. Pritchard, A. Blake, A.R. Peacocke, Modified intercalation model for the interaction of amino acridines and DNA, Nature 212 (1966) 1360–1361.
[46] J. Rupar, M. Aleksić, V. Dobričić, O. Čudina, J. Brborić, S. Vladimirov, Application of electrochemical biosensor for investigation of acridine derivatives - DNA interaction, in: 14thInternational Conf. Fundam. Appl. Asp. Phys. Chem. B. Proc., Belgrade, 2018: pp. 379–382.

[47] V.C. Diculescu, M. Vivan, A.M. Oliveira Brett, Voltammetric behavior of antileukemia drug glivec. Part III: In situ DNA oxidative damage by the glivec electrochemical metabolite, Electroanalysis. 18 (2006) 1963–1970, https://doi.org/10.1002/elan.200603602.
[48] M.-C. Bunea, V.-C. Diculescu, M. Enculescu, H. Iovu, T.A. Enache, Redox mechanism of azathioprine and its interaction with DNA, Int. J. Mol. Sci. 22 (2021) 6805, https://doi.org/10.3390/ijms22136805.
[49] A.M. Oliveira-Brett, V.C. Diculescu, Electrochemical study of quercetin-DNA interactions: Part II, In situ sensing with DNA biosensors, Bioelectrochemistry. 64 (2004) 143–150, https://doi.org/10.1016/j.bioelechem.2004.05.002.
[50] Y. Temerk, M. Ibrahim, H. Ibrahib, W. Schuhmann, Comparative studies on the interaction of anticancer drug irinotecan with dsDNA and ssDNA, RSC Advances 8 (2018) 25387–25395, https://doi.org/10.1039/C8RA03231A.
[51] Q. Feng, N.-Q. Li, Y.-Y. Jiang, Electrochemical studies of porphyrin interacting with DNA and determination of DNA, Anal. Chim. Acta. 344 (1997) 97–104, https://doi.org/10.1016/S0003-2670(97)00008-1.
[52] J. Sochr, K. Nemčeková, M. Černicová, K. Campbell, V. Milata, D. Farkašová, J. Labuda, DNA Interaction with 17α-Ethinylestradiol Studied Using Electrochemical Biosensors and Biosensing in Solution, Electroanalysis. 31 (2019) 1961–1968, https://doi.org/10.1002/elan.201900091.
[53] S. Ramotowska, A. Ciesielska, M. Makowski, What can electrochemical methods offer in determining DNA–drug interactions? Molecules. 26 (2021) 3478, https://doi.org/10.3390/molecules26113478.
[54] Y. Yardım, M. Vandeput, M. Çelebi, Z. Şentürk, J.M. Kauffmann, A Reduced Graphene Oxide-based Electrochemical DNA Biosensor for the Detection of Interaction between Cisplatin and DNA based on Guanine and Adenine Oxidation Signals, Electroanalysis. 29 (2017) 1–9, https://doi.org/10.1002/elan.201600804.
[55] N.H. Moghaam, S. Salehzadeh, N. Shahabadi, Spectroscopic and molecular docking studies on the interaction of antiviral drug nevirapine with calf thymus DNA, Nucleosides Nucleotides Nucleic Acids. 36 (2017) 1–18, https://doi.org/10.1080/15257770.2017.1346800.
[56] A. Chakraborty, A.K. Panda, R. Ghosh, I. Roy, A. Biswas, Depicting the DNA binding and photo-nuclease ability of anti-mycobacterial drug rifampicin: A biophysical and molecular docking perspective, Int. J. Biol. Macromol. 127 (2019) 187–196, https://doi.org/10.1016/j.ijbiomac.2019.01.034.
[57] N. Shahabadi, Z.M. Kalar, A. Veysi-Rayegani, DNA interaction studies of an antiviral drug, ribavirin, using different instrumental methods, DNA Cell Biol. 31 (2012) 876–882, https://doi.org/10.1089/dna.2011.1456.
[58] S. Ponkarpagam, G. Mahalakshmi, K.N. Vennila, K.P. Elango, Multi-spectroscopic, voltammetric and molecular docking studies on binding of anti-diabetic drug rosigiltazone with DNA, Spectrochim. Acta - Part A Mol, Biomol. Spectrosc. 234 (2020), 118268, https://doi.org/10.1016/j.saa.2020.118268.
[59] K. Morawska, T. Popławski, W. Ciesielski, S. Smarzewska, Electrochemical and spectroscopic studies of the interaction of antiviral drug Tenofovir with single and double stranded DNA, Bioelectrochemistry. 123 (2018) 227–232, https://doi.org/10.1016/j.bioelechem.2018.06.002.
[60] S. Nafisi, A.A. Saboury, N. Keramat, J.F. Neault, H.A. Tajmir-Riahi, Stability and structural features of DNA intercalation with ethidium bromide, acridine orange and methylene blue, J. Mol. Struct. 827 (2007) 35–43, https://doi.org/10.1016/j.molstruc.2006.05.004.
[61] R. Hajian, P. Hossaini, Z. Mehrayin, P.M. Woi, N. Shams, DNA-binding studies of valrubicin as a chemotherapy drug using spectroscopy and electrochemical techniques, J. Pharm. Anal. 7 (2017) 176–180, https://doi.org/10.1016/j.jpha.2017.01.003.
[62] E. Jabeen, N.K. Janjua, S. Ahmed, I. Tahiri, M. Kashif, A. Javed, DNA binding interaction studies of flavonoid complexes of Cu(II) and Fe(II) and determination of their chemotherapeutic potential, Inorganica Chim. Acta. 496 (2019), 119048, https://doi.org/10.1016/j.ica.2019.119048.
[63] A. Adams, J.M. Guss, C.A. Collyer, W.A. Denny, A.S. Prakash, L.P.G. Wakelin, Acridinecarboxamide topoisomerase poisons: Structural and kinetic studies of the DNA complexes of 5-substituted 9-amino-(N-(2-dimethylamino)ethyl)acridine-4-carboxamides, Mol. Pharmacol. 58 (2000) 649–658, https://doi.org/10.1124/mol.58.3.649.